

Synthesis, Characterization, and Adsorptive Characteristics of Radiation-Grafted Glycidyl Methacrylate Bamboo Fiber Composites

Ruqayya Shaheen, Tariq Yasin, Zarshad Ali,* Amir Sada Khan, Bushra Adalat, Mehwish Tahir, and Sher Bahadar Khan



Cite This: *ACS Omega* 2023, 8, 38849–38859



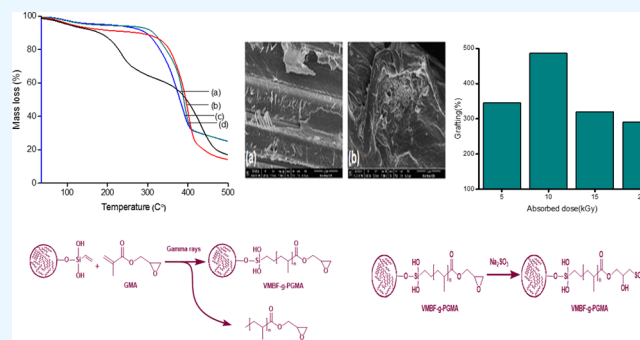
Read Online

ACCESS |

Metrics & More

Article Recommendations

ABSTRACT: In the present study, a biosorbent was prepared through the radiation-induced graft polymerization (RIGP) technique by using a glycidyl methacrylate (GMA) monomer. Functionalized bamboo materials were used for grafting. The grafting percentage (G %) of GMA on bamboo fibers was assessed based on the optimization of the absorbed dose and concentration of the monomer. The chemical modification of the polymerized product into the sulfonated form of the grafted biopolymer was carried out by using sodium sulfite solution. The modification of the biopolymer at various stages was analyzed by Fourier transform infrared (FTIR) spectroscopy and X-ray diffraction (XRD) techniques. By performing scanning electron microscopy (SEM), the morphological changes of the prepared biopolymer were analyzed. The temperature stability of the synthesized material was assessed by the thermogravimetric analysis (TGA) technique. The prepared sulfonated biosorbent was used in the batch adsorption study for the uptake of copper. We examined a variety of variables, including pH, adsorbent dosage, and time. The adsorption kinetics were studied using pseudo-first-order (PFO) and pseudo-second-order (PSO) models. Adsorption isotherms and thermodynamic parameters were also applied to study the adsorption capacity of the biosorbent. The maximum copper adsorption capacity was found to be 198 mg g^{-1} from the Langmuir isotherm. Copper adsorption followed PSO kinetics ($R^2 = 0.999$). This inexpensive and eco-friendly biosorbent removed 96% of copper ions from the solution.



1. INTRODUCTION

Natural polymers or biopolymers are derived from renewable resources found in living organisms, such as plants, animals, and microorganisms. Cellulose, collagen, proteins, starch, chitin, etc., are common examples of abundantly available natural polymers. Indeed, biopolymers have garnered significant attention in various industrial and biomedical applications due to their remarkable properties.¹ They are biocompatible, nontoxic, renewable, cheap, easily accessible, and have no adverse effects on living organisms or the environment.² Polymers can be modified through various techniques to enhance their stability, flexibility, and solubility as well as to introduce new properties. Some of the common techniques used for polymer modification include blending, cross-linking, and composite formation.³ Among these techniques, researchers have focused on the grafting phenomenon to enhance the properties of various materials, including polymers. Grafting involves the covalent attachment of polymer chains to the surface of a base material. This process can lead to significant improvements in the surface properties, stability, and functionality of the material.⁴

In recent years, simultaneous radiation grafting has been an attractive and versatile method used to introduce functional groups onto the surface of a substrate. It involves the initiation of free radicals on monomers in the presence of the substrate using ionizing radiation sources, such as γ rays, ultraviolet (UV) light, or electron beams. These free radicals then react with the substrate, leading to the grafting of the monomer onto its surface.⁵ Radiation-induced graft polymerization is a valuable technique for developing grafted polymers with various advantages. Bulk grafting through radiation-assisted methods offers several benefits, making it an efficient, accurate, simple, and environmentally friendly approach to the modification of polymeric materials. One of the significant advantages of simultaneous radiation grafting is that it does not

Received: April 11, 2023

Accepted: September 29, 2023

Published: October 13, 2023



require the use of solvents, initiators, or high temperatures. The initiation of free radicals occurs directly on the monomer molecules through ionizing radiation, eliminating the need for additional chemicals or energy-intensive conditions. The advantage of this technique is that newer homopolymers are produced. The optimization of the “monomer concentration” and “absorbed dose” is important to achieve maximum grafting percentage.⁶ Glycidyl methacrylate is a remarkable functional monomer that has numerous properties as an ion-exchange resin.⁷ The structure of glycidyl methacrylate (GMA) is advantageous as it has not only vinyl groups but also a pendant epoxy group with the ability of ring-opening reactions. The pendant epoxy group in GMA also has the capacity to undergo postpolymerization modifications, which facilitates the conversion of inert functional groups of the monomers into a variety of required “functional groups”.⁸ Elkady et al., used a polymethacrylate-grafted nanosulfonated material as a cation exchanger to successfully remove Cd(II) ions from wastewater.⁹ Hus et al., prepared pGMA by the polymerization of phase emulsions for the removal of silver and lead ions from solutions.¹⁰ Korpayev et al., grafted GMA onto a polypropylene/polyethylene nonwoven fabric through radiation grafting and further modified with ethylenediamine for efficient adsorption of As(v). LV et al., synthesized polyaniline composites with various natural waste materials, such as hazelnut shells, walnut, etc., for the adsorption of Cr(VI) ions from aqueous solutions.¹¹

Currently, the use of biocomposite materials has increased, and the bamboo plant occupies a particular position among them. Natural fibers have extended substantially as opposed to synthetic ones as they are biodegradable and widely available.¹² Natural fibers possess unique surface properties that make them effective adsorbents for various pollutants. In addition, these cheap biofibers have numerous environmental benefits over synthetic fibers when used as a reinforcement. Because of their enhanced mechanical qualities, higher surface area, and higher adsorption capacity, bamboo fibers are employed as reinforcements in composite materials.¹³ Their hydroxyl functionality makes them suitable as basic materials for the grafting of other materials.¹⁴ Cichoż et al., prepared biopolymers by the chemical grafting of acrylic acid onto bamboo rayon by using KPS as an initiator.¹⁵ Various kinds of organic and inorganic contaminants in wastewater effluents have been reported and their excess concentration is known to be toxic for aquatic organisms.¹⁶ Various adsorbents, including carbon adsorbents, biopolymers, and hydrogel adsorbents, are essential for pollutant removal in various environmental and industrial applications.¹⁷ Heavy metals are major inorganic pollutants. Various industries such as textiles, plumbing, fertilizer, electroplating, and leather release different metals.¹⁸ The metals containing effluents, when discharged into waterbodies, pollute the aquatic environment and accumulate within the food chain. Heavy metals such as copper may even cause death at high concentrations in human beings. Various methods have been applied for the elimination of toxic metals, but most of them have serious restrictions and are expensive. Therefore, the development of low-cost, efficient,¹⁹ simple, and eco-friendly adsorbents are extremely attractive to remove toxic metals from wastewater.²⁰

The current work focuses on utilizing a glycidyl methacrylate (GMA)-grafted biopolymer by using a simultaneous radiation-grafting method, a novel approach that has not been previously reported in the literature. The main objective is to optimize the

influence of the absorbed dose and monomer concentration during the grafting process. The chosen substrate for grafting is bamboo fiber, which is a natural biopolymer with unique properties. The grafted bamboo fiber, obtained through simultaneous radiation grafting of GMA, is then further chemically modified to the sulfonated form using a postpolymerization technique. This sulfonated form enhances the affinity and capability of the material to adsorb copper ions from aqueous solutions. The grafted biopolymer is characterized by attenuated total reflectance fourier transform infrared (ATR-FTIR) spectroscopy, scanning electron microscopy (SEM), thermogravimetric analysis (TGA), and X-ray diffraction (XRD) techniques.

2. EXPERIMENTAL

2.1. Materials and Methods. Glycidyl methacrylate (GMA), vinyl triethoxysilane (VTES), hydrochloric acid (HCl 37%), methanol (CH₃OH), isopropanol (CH₃)₂CHOH, and acetone (CH₃)₂CO were acquired from Sigma-Aldrich, Germany. Tween 80 was procured from Riedel-Haën, Germany.

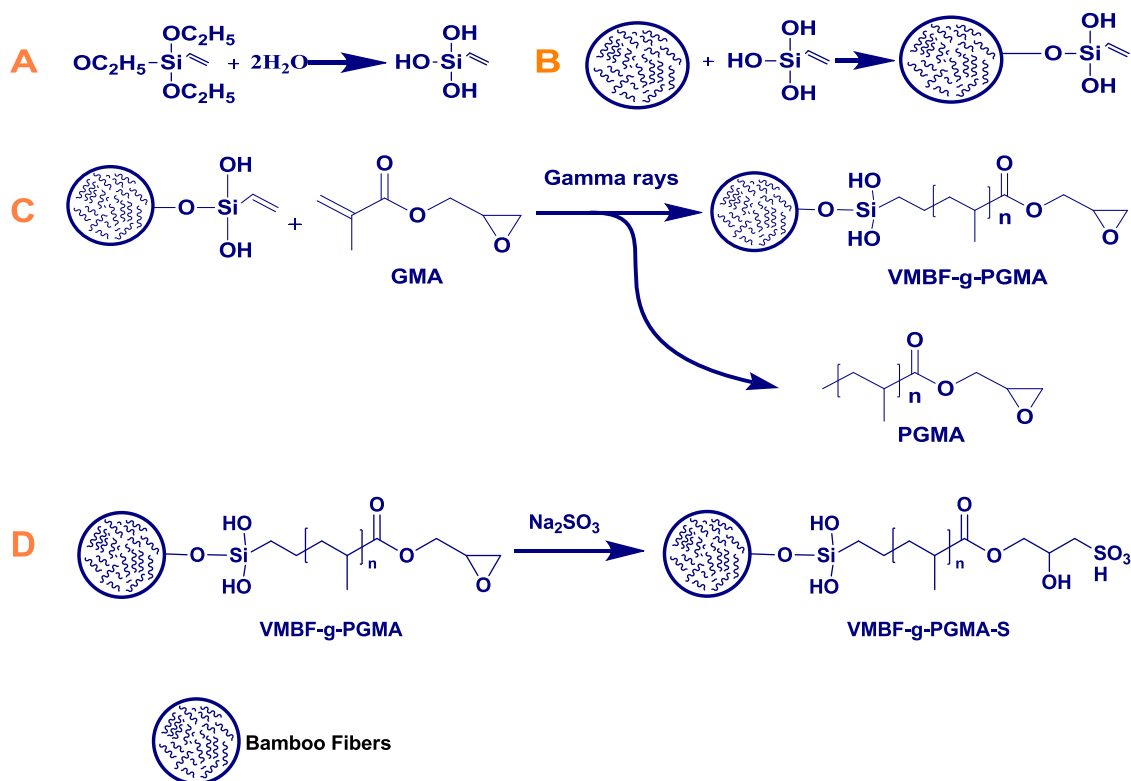
2.2. Synthesis of the Biosorbent. **2.2.1. Radiation Polymerization of GMA on Bamboo Fibers.** Using the reported method,¹⁵ vinyl-modified bamboo fibers (VMBFs) were prepared in a glass reactor containing 10 g of bamboo fibers and isopropanol solution. After that, the mixture was hydrolyzed by the dropwise addition of VTES. At 60 °C, the mixture was stirred for 2 h. The resulting mixture was filtered, rinsed with methanol, and vacuumdried. For the formation of a stable suspension, the vinyl-modified bamboo fibers (VMBFs) (1 g) were dispersed into a flask (100 mL) in deionized water and then stirred for 1 h under an inert environment. After that, the GMA monomer was added to the solution mixture, and the vials were sealed and purged with nitrogen gas. A Cobalt-60 γ irradiator was used for irradiation (24 kCi, 2.5 kGy/h). The grafting yield was monitored at different absorbed doses (5–20 kGy). For the purpose of removing unreacted monomers and the homopolymer, the grafted product was washed with acetone. The washed sample was dried at 60 °C until “constant weight” and was named VMBF-g-PGMA. The following equation was used to compute the grafting percentage (%) of VMBF-g-PGMA.

$$G\% = \frac{W_g - W_o}{W_o} \times 100 \quad (1)$$

Here, W_o indicates the weight of VMBF, and W_g is the weight of VMBF-g-PGMA.

2.2.2. Sulfonation of the VMBF-g-PGMA Biosorbent. For sulfonation, the sulfonic acid groups were incorporated into VMBF-g-PGMA. 0.1 g of VMBF-g-PGMA was dispersed in Na₂SO₃/isopropyl alcohol/water with 1.3:1:1.7 (13:10:77) volume ratio, and the resulting mixture was refluxed at 80 °C. After 6 h, the sulfonated mixture was treated with 1 M HCl overnight under stirring, and the sodium form (–SO₃Na) of the biopolymer was converted into SO₃H–. Using acetone, the obtained sample was washed and dried at 60 °C. A gravimetric analysis was performed to determine the molar ratio of (SO₃H–) group to “GMA” units by using eq 2²¹

$$\frac{\eta_{\text{SO}_3\text{H}}}{\eta_{\text{GMA}}} = \frac{(W_s - W_g)\text{MGMA}}{(W_g - W_o)\text{MSO}_3} \quad (2)$$

Scheme 1. Steps Involved in the Synthesis of the Sulfonated Biopolymeric Material^a

^aHydrolysis of silane (A); vinyl modification of bamboo fibers (B); radiation-induced grafting (C); and sulfonation (D)

Here, W_o = material weight before grafting; W_g = material weight after grafting; W_s = sulfonated material weight; GMA and SO_3 units have molar weights of 142.15 and 80 g mol^{-1} , respectively.

2.3. Batch Adsorption Study of copper. For metal adsorption experiments, a stock solution was prepared by mixing 1000 mg of copper sulfate in deionized water (1 L). Samples of different copper concentrations were prepared. The Cu(II) solutions were added to the sulfonated biosorbent. At 800 rpm, the resultant mixture was centrifuged for 4 h. The desired pH of the solution was maintained by adding 0.01 M HCl or NaOH solutions, respectively, using a pH meter (Hanna HI-2211 pH/ORP). The absorbance of the prepared sample solutions upon copper adsorption was analyzed by using an atomic absorption spectrophotometer. The adsorbed quantity of copper “per unit mass” on radiation-grafted sulfonated bamboo fibers was measured using eqs 3 and 4.

$$Q = \left[\left(\frac{C_i - C_e}{m} \right) \right] \times V \quad (3)$$

Here, “ C_i ” (mg) and “ C_e ” denote initial and equilibrium copper concentrations (mg L^{-1}), respectively. “ V ” is the volume of the metal ion solution, and “ M ” is the mass of the adsorbent (grams). The removal percentage ($R\%$) of copper ions after adsorption was calculated using eq 4.

$$\text{removal (\%)} = \left[\left(\frac{C_i - C_e}{C_i} \right) \right] \times 100 \quad (4)$$

2.4. Characterization. A Thermo Electron Corporation FTIR-ATR (Nicolet 6700) spectrophotometer was used for the detection of various functional groups. The samples were

scanned with an 8 cm^{-1} resolution between 400 and 500 cm^{-1} . Using a Discover X-ray diffractometer (D8), XRD was performed at room temperature. The diffractograms were obtained for 2θ values of $5\text{--}80^\circ$. The X-ray beam used nickel-filtered $\text{Cu K}\alpha$ ($\lambda 1/4$ 1.542 Å) radiation, which worked at 30 kV and 30 mA. The change in the structural morphology of the grafted biosorbent was examined by using field-emission SEM (TESCAN MIRA-3). Before scanning, the amorphous surface of the samples was made conductive before scanning. Thermogravimetric measurements were performed by using a Mettler Toledo TGA/DSC1 TGA analyzer. The flow rate of nitrogen was kept at 50 mL min^{-1} from room temperature to 600°C .

3. RESULTS AND DISCUSSION

3.1. Synthesis of the Sulfonated Biopolymer. Bamboo fibers were silanized using vinyl triethoxysilane as a coupling agent. VTES has one vinyl group and three ethoxy groups. Bamboo fibers containing acidified 2-propanol solution will hydrolyze the alkoxy groups into active silanol groups. The “silanol groups” reacted with other silanol groups of neighboring fibers to produce Si–O–Si linkages. When exposed to radiation, GMA monomers become acceptors of VMBF radicals by initiating a chain reaction to produce VMBF \cdot and GMA \cdot .²² In the polymerization step, VMBF \cdot and GMA \cdot polymerize to form VMBF-g-PGMA and the PGMA chain. Finally, during sulfonation, sodium sulfite was used to convert the epoxy group of the grafted polymers into a sulfonated form by a ring-opening reaction, as shown in Scheme 1.

3.2. Parameter Optimization. **3.2.1. Influence of the Absorbed Dose on Grafting (%).** The optimization of the

absorbed dose is vital to obtain the maximum grafting yield. As shown in Figure 1(a), samples of the same composition, i.e.,

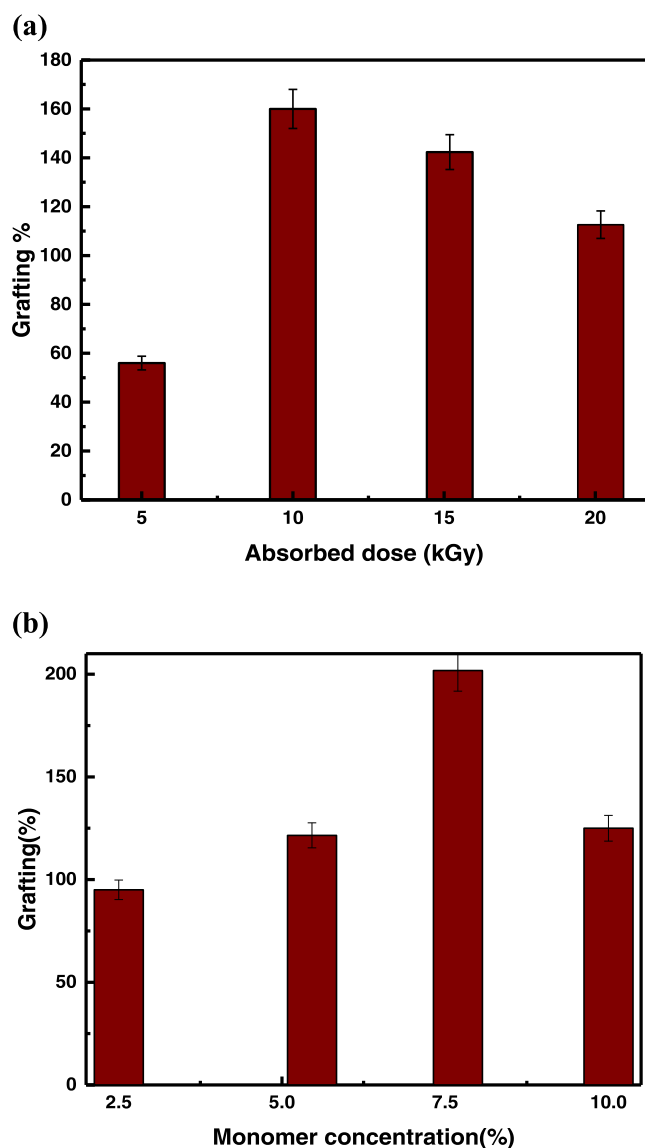


Figure 1. (a) Effect of the absorbed dose (5–20 kGy) on the degree of grafting (%) for the radiation-induced grafting of GMA onto bamboo fibers at 5% monomer concentration and 2.5 kGy/h dose rate. (b) Effect of the monomer concentration (2.5–10%) on the degree of grafting (%) for the radiation-induced grafting of GMA onto bamboo fibers at 10 kGy absorbed dose and 2.5 kGy/h dose rate

1% VMBF and 5% GMA, were exposed to radiation at an absorbed dose rate of 5–20 kGy. The Figure shows that the grafting percentage (G %) reaches a maximum (160%) at 10 kGy, which may be due to the generation of free radicals on the monomer and polymer backbone. Hence, an absorbed dose of 10 kGy was selected for further studies. After 10 kGy, the cross-linked product was formed in the reaction mixture, and the degree of grafting percentage decreased by increasing the absorbed dose.²² Similar findings have been reported by Taimur et al., for copper ion adsorption by using the radiation-grafting method on amidoxime-based nanohybrid materials, and the maximum grafting % was found to be 280% at 5 kGy.²³

3.2.2. Effect of the Monomer Concentration on Grafting (%). At a constant absorbed dose of 10 kGy, the effect of a

change in the “monomer concentration” on the grafting percentage (%) was investigated. The monomer amount was changed from 2.5 to 10%, as displayed in Figure 1(b). The obtained results show that the grafting yield first increases rapidly up to 202% with increasing concentration of GMA up to 7.5% and then slightly decreases on further increasing the monomer concentration.²⁴ Initially, free radical formation enhanced the grafting percentage, while later, homopolymerization caused a decline in the grafting percentage and made the monomer approach toward grafted chains.²⁵ The dependence of the grafting percentage on the concentration of the monomer was also reported in earlier studies and it was observed that 5% monomer (GMA) concentration leads to the highest grafting of 665% by RIGP of GMA onto sepiolite.²¹

3.3. ATR-FTIR Analysis. Figure 2 displays the ATR-FTIR spectra of bamboo fibers and the VMBFs formed via the

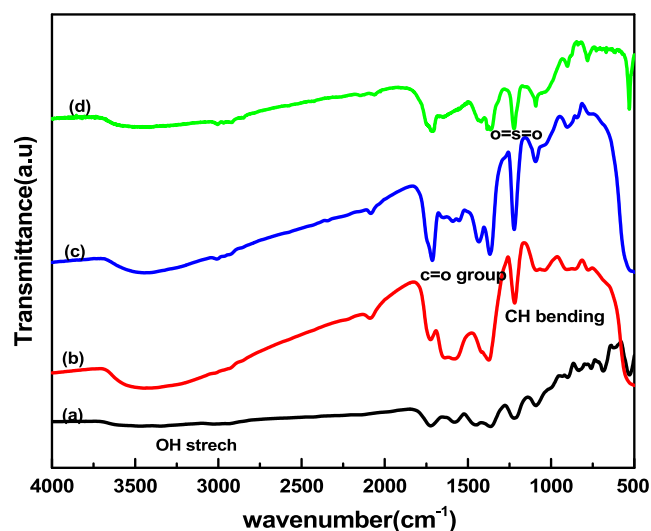


Figure 2. ATR-FTIR spectra of (a) RBF, (b) VMBF, (c) VMBF-g-PGMA, (d) and VMBF-g-PGMA-S samples

grafting of GMA and sulfonation. The characteristic peak at 3665–3013 cm⁻¹ was observed due to the vibrational stretch of the OH group. The stretching of the (C=O) group of pectin and hemicellulose was observed in the range of 1765–1612 cm⁻¹.²⁶ At 1514 cm⁻¹, the vibrational stretching of C=C in the aromatic ring of lignin was detected.²⁷ The silanized bamboo fibers exhibited a peak at 2971 cm⁻¹ because of CH stretching. The peaks at 1259, 1365, and 1487 cm⁻¹ are attributed to CH bending vibrations. The Si–O vibrations were observed at 979 and 771 cm⁻¹.²⁸ In GMA-grafted bamboo fibers, the cellulose region is extremely reduced due to the consumption of the most OH sites present on the backbone of the polymer by “GMA” molecules. The formation of ‘poly (GMA)’ chains, which elongated from the stem polymer, eventually covered the whole fibers at a higher grafting yield. This makes the C–H and C–O band detection more difficult on grafted fibers. This also signifies the incorporation of GMA molecules onto the cellulose backbone. The spectrum shows the presence of a peak at 1732 cm⁻¹, which reflects the presence of the (–C=O) group of GMA. Epoxy group vibrations were observed at 1255 and 952–848 cm⁻¹. This indicates that the GMA was successfully incorporated onto bamboo fibers.²⁹ A small peak of the sulfonate group appeared at 1152 cm⁻¹ and increased in

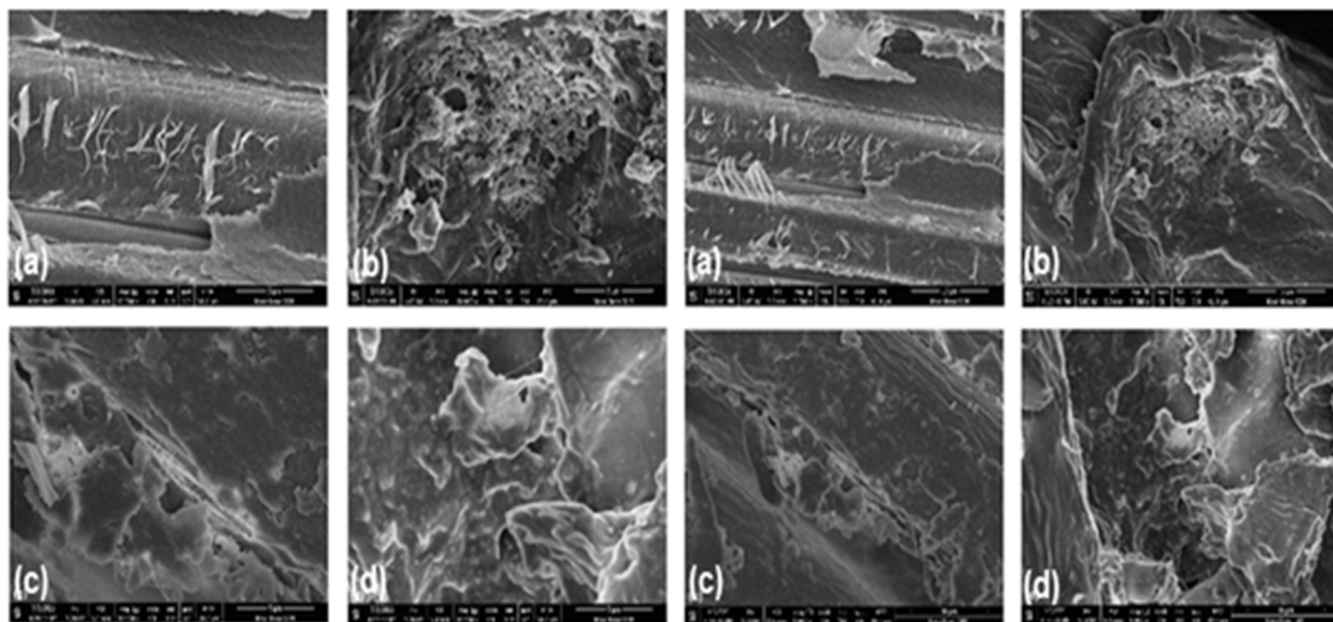


Figure 3. SEM micrographs of glycidyl methacrylate-grafted bamboo fibers using radiation-induced graft polymerization: (a) RBF, (b) VMBF, (c) VMBF-g-PGMA, and (d) VMBF-g-PGMA-S at 5 and 10 μm , respectively

intensity at 1288 and 670 cm^{-1} , indicating successful sulfonation.³⁰

3.4. SEM Analysis. By using SEM analysis, the morphological changes in raw bamboo fibers and their different grafted forms were studied, and the morphological changes are displayed in Figure 3. Figure 3(a) shows that the surface of untreated bamboo fibers is smooth, with a rod-like dense network structure, and is accompanied by a superficial layer of impurities.³¹ The micrograph of VMBF (Figure 3b) reveals that a drastic change occurred in the surface morphology of fibers due to the mercerization process, which leads to the breakage of fibers into smaller fibers with rough surfaces. The silane modification of bamboo fibers with VTES and the incorporation of vinyl groups are also attributed to the change in morphology.³² Figure 3(c) of VMBF-g-PGMA confirms that the surface of pretreated bamboo fibers is further disaggregated, which facilitates the reaction with the GMA monomer. All fibers were completely incorporated into the GMA monomer due to the formation of a GMA copolymer layer onto fibers.³³ The sulfonation changes the surface morphology of VMBF-g-PGMA, as displayed in Figure 3(d). The fibers retained their fibril-like morphology and became shorter, thinner in diameter, and less bundled. The result shows that the structural integrity of bamboo fibers was retained in their modified forms because of the functionalization of the fiber surface.³⁴ The size of the sulfonated biosorbent was observed to be 15 μm .

3.5. XRD Analysis. Figure 4 displays the XRD diffractograms of RBF, VMBF, VMBF-g-PGMA, and VMBF-g-PGMA-S. The peak of the untreated bamboo fiber at $2\theta = 22.3^\circ$ shows the reflections of the cellulose lattice planes. The two weaker diffraction peaks at 2θ angles between 13 and 17° were also observed.³⁵ A decrease in the peak intensity and crystallinity was observed after silanization. Because of the reflections of organosilane units of VTES, the peaks at 16.8 and 13.8°, along with small peaks at 26.5, 34.7, and 36.8°, were observed.³⁶ Grafting of “GMA” onto “VMBF” caused an increase in the peak intensity at 14–17°, which supports the grafting of GMA

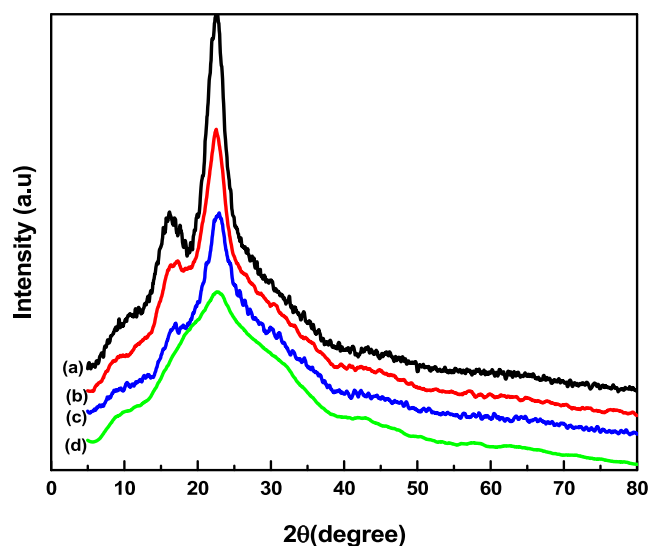


Figure 4. X-ray diffraction patterns of (a) RBF, (b) VMBF, (c) VMBF-g-PGMA, and (d) VMBF-g-PGMA-S samples

on VMBF.³³ An increase in the amorphous phase after sulfonation of VMBF-g-PGMA was observed by a decrease in the peak height in comparison to that of VMBF due to the incorporation of amorphous organic groups (SO_3H) and also an increase in the interchain distances.³⁷

3.6. TGA Analysis. The thermal stability and decomposition of RBF, VMBF, VMBF-g-PGMA, and VMBF-g-PGMA-S are displayed in Figure 5. The thermogram of raw bamboo fibers (RBF) showed that up to 150 $^\circ\text{C}$, there is an estimated 22% mass loss due to the elimination of absorbed water due to the hydrophilic nature of lignocellulose fibers.³⁸ It was observed that after treatment with alkali and the silanization of bamboo fibers with VTES, the hydrophilicity of bamboo fibers reduced significantly. This tends to increase the stability of modified bamboo fibers.³⁹ VMBF exhibits only a single-step degradation profile in the range of 270–340 $^\circ\text{C}$

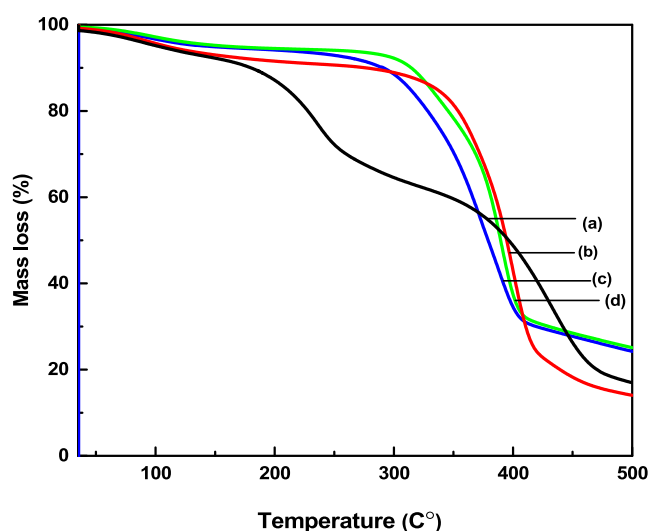


Figure 5. TGA micrographs: (a) RBF, (b) VMBF, (c) VMBF-g-PGMA, and (d) VMBF-g-PGMA-S samples

due to the cellulose and hemicellulose decomposition behavior. The TGA curves of VMBF-g-PGMA exhibit a higher thermal stability of developed biopolymer due to the formation of higher-molecular-weight polymers.⁴⁰ Because of the removal of water from ambient temperature to 120 °C, the first mass loss occurred. The second mass loss was observed from 120 to 286 °C because of the decomposition of pendent groups. A continuous mass loss above 320 °C occurred as a result of the breakdown of high molecular weight polymer chains. The hydrophilic nature of sulfonation improved the thermal stability of VMBF-g-PGMA-S.

3.7. Adsorption Studies of Copper. 3.7.1. Effect of pH.

Figure 6 shows how the pH influences the Cu(II) ion

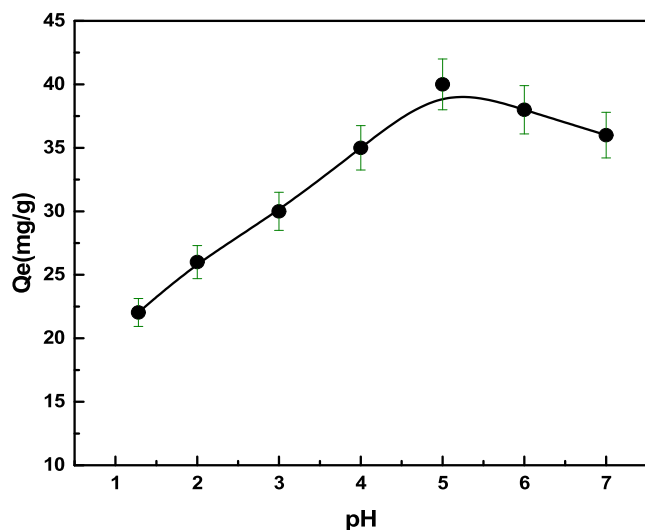


Figure 6. Effect of “pH” on the removal of Cu(II) ions by VMBF-g-PGMA-S; $C_0 = 20 \text{ mg L}^{-1}$; volume = 20 mL; and $T = 293 \text{ K}$

adsorption on the sulfonated biosorbent. At pH 5, a significant increase in the adsorption capacity (40 mg g^{-1}) for copper(II) ions was observed. At low pH, the VMBF-g-PGMA-S capacity to chelate copper ions was lower. At pH 5, the deprotonation of the sulfonic group produced active sites that form complexes with Cu(II) ions. Cu(II) ions are more vulnerable to (OH^-)

ions and form “ $\text{Cu}(\text{OH})_2$ ” precipitates in solutions at higher pH levels because adsorbents have a lower capacity for Cu(II). In order to avoid precipitation, further adsorption studies were conducted at pH 5.⁴¹ Singa and Guleria found that for the adsorption of Cu(II) ions by poly(acrylonitrile-co-methacrylic acid)-g-cellulosic okra polymers, the maximum adsorption capacity was observed at pH 5.5–6.5.⁴²

3.7.2. Effect of the Adsorbent Content. **Figure 7** illustrates the influence of the adsorbent dose on the removal percentage (%) and on the adsorptive capacity (mg g^{-1}) of Cu(II). Because of the aggregation of particles, a decreasing trend of Q_e was observed on increasing the amount of the adsorbent.⁴³ Moreover, the results also showed that the percentage removal of Cu(II) ions increased as the adsorbent quantity was increased. This was mainly because of the presence of specific exchange sites and the surface area on VMBF-g-PGMA-S, which leads to 96% adsorption. A novel cellulose-g-acrylic acid copolymer was prepared by Hajeeth et al., who tested its ability for Cu(II) ion adsorption. A maximum of 75.5% removal was achieved by varying the adsorbent contents.⁴⁴

3.7.3. Contact Time and Evaluation of Adsorption Kinetics. At different time intervals, the variation in the adsorption capacity of Cu(II) ions was examined, and the results are displayed in **Figure 8(a)**. The adsorption capacity increased rapidly up to 60 min and then became lower after 60 min until the adsorption equilibrium was achieved after 90 min. This may be due to the fact that at the initial stages, the metal uptake was extremely high due to the presence of vacant sites on adsorbents, and later on, the uptake decreased because more adsorbate molecules migrated toward the adsorbent and the vacant sites got occupied.⁴⁵ The results of our study for the adsorption of Cu(II) ions from aqueous solution are consistent with Cu(II) adsorption on bioballs previously reported.⁴⁶

The adsorption process is key to understanding the effects of an adsorbent on the metal adsorption capacity. Kinetic models such as pseudo-first-order and pseudo-second-order models are used to interpret the adsorption kinetics as given in **eq 5**.

$$\frac{dQ_t}{dt} = k_1(Q_e - Q_t) \quad (5)$$

where “ Q_t ” represents the quantity of adsorbate adsorbed at time “ t ” and “ Q_e ” at equilibrium. “ t ” represents the contact time, while “ k_1 ” is the pseudo-first-order rate constant.⁴⁷ The pseudo-first-order kinetics in the linear integral form can be expressed as **eq 6**

$$\log(Q_e - Q_t) = \log Q_e - k_1 2.303t \quad (6)$$

where the $\log(Q_e - Q_t)$ versus “ t ” plot shows a linear form. The slope and intercept of the plot are used to determine the values of k_1 and Q_e , respectively, and **eq 7** shows the pseudo-second-order differential form

$$dQ_t/dt = k_2(Q_e - Q_t)^2 \quad (7)$$

here, K_2 = pseudo-second-order rate constant; the simplified form of **eq 7** is shown as **eq 8**

$$t/Q_t = 1/k_2 Q_e + t/Q_t \quad (8)$$

The linear relationship is obtained from the t/Q_t versus “ t ” plot. The intercept and slope of the plot are used to compute the values of k_2 and Q_e , respectively.⁴⁸ **Figure 8(b,c)** displays the experimental results of both kinetic models. **Table 1** represents the kinetic parameters of Cu(II) ion adsorption on

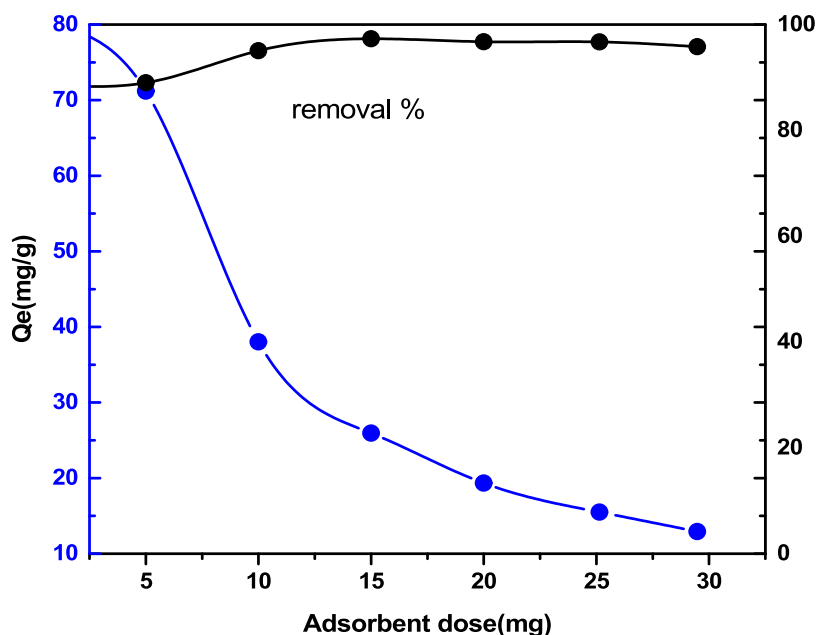


Figure 7. Effect of the “adsorbent quantity” on the removal of the Cu(II) ions by VMBF-g-PGMA-S (mass = 5–25 mg; Co = 20 mg L⁻¹; volume = 20 mL; and T = 293 K).

VMBF-g-PGMA-S for both pseudo-first-order and pseudo-second-order models. The PSO modeling affords the best explanation for Cu(II) ion adsorption onto the sulfonated biosorbent. Correlation coefficients (R^2) and Q_e of the kinetic model are well described by the PSO model. Therefore, it is concluded that adsorbents undergo a chemisorption process.⁴⁹ Kumar et al., have reported analogous results for the adsorption of Cu(II) ions by using the cellulose-grafted glycidyl methacrylate monomer and found that the adsorption kinetics followed a pseudo-second-order model.⁵⁰

3.7.4. Initial Concentration and Adsorption Isotherms. Figure 9(a) shows that at low initial concentrations, the adsorption of Cu(II) ions was found to increase faster. The adsorption capacity was maximum at 100 mg L⁻¹. The adsorption capacity was higher at lower concentrations because of the interaction of Cu(II) ions in solution with active sites of the adsorbent. As the adsorption sites become saturated at higher concentrations, the adsorption capacity decreases.⁵¹ The favorability of the adsorption process was analyzed by the Langmuir and Freundlich isotherms.⁵² The Langmuir isotherms can be explained by using eq 9

$$1/Q_e = 1/k_L Q_m 1/C_e + 1/Q_m \quad (9)$$

Here, Q_e denotes the adsorption capacity at equilibrium (mg·g⁻¹). The monolayer adsorption of adsorbents is expressed as Q_m (mg·g⁻¹). The equilibrium concentration is C_e , while K_L is associated with the free energy of adsorption related to the Langmuir constant (L mg⁻¹). The Freundlich isotherm was determined using eq 10

$$\ln Q_e = \ln k_f + 1/n \ln C_e \quad (10)$$

The Freundlich constant “ K_F ” shows the Freundlich adsorption capacity, while “ n ” represents the intensity of adsorption. A value of “ n ” between 2 and 10 indicates good sorption. The values between 1 and 2 indicate moderate sorption, while a value <1 indicates poor sorption.⁵³ A comparison of the higher value of correlation coefficients (R^2) for both adsorption isotherms in Figure 9(b,c) and Table

2 reveals that the Langmuir isotherm best describes the experimental data. Moreover, it also demonstrates the monolayer adsorption of Cu(II) ions onto binding sites of VMBF-g-PGMA-S having uniform energies of adsorption. The removal of Cu(II) ions by the graft copolymerization of acrylamide onto chitosan was also investigated by Al-Karawai et al., and the adsorption process was found to obey the Langmuir isotherm.⁵⁴

3.7.5. Thermodynamic Parameters. To assess the favorability of adsorption, many thermodynamic functions (ΔG° , ΔH° , and ΔS°) are used. Equation 11 is used to calculate the Gibbs free energy (ΔG°).

$$\Delta G = -RT \ln K_D \quad (11)$$

$$K_D = \frac{C_o - C_e}{\left(\frac{ms}{V}\right)C_e} \quad (12)$$

By using the Van't Hoff eq (eq 13), the standard enthalpy change was calculated

$$\ln K_D = \frac{\Delta S}{R} - \frac{\Delta H}{RT} \quad (13)$$

The slope of $\ln K_D$ versus $1/T$ is used to calculate ΔH° . The intercept of the $\ln K_D$ versus $1/T$ plot is used to determine the value of ΔS° . In Table 3, the negative values of ΔG° and ΔH° show that the adsorption process was spontaneous and exothermic. Moreover, the positive value of ΔS° shows that the adsorbent material does not undergo any significant structural changes.⁵⁵ Similar results were also obtained by Kumar et al. for Cu(II) ion adsorption by using poly(HEMA-co-AAc)-grafted cellulose.⁵⁰

4. CONCLUSIONS

Novel VMBF-g-PGMA-S-grafted biopolymers were synthesized by RIGP of GMA monomers onto bamboo fibers. The VMBF and GMA monomers were irradiated at 10 kGy (absorbed dose) and 7.5% (concentration of monomer). The

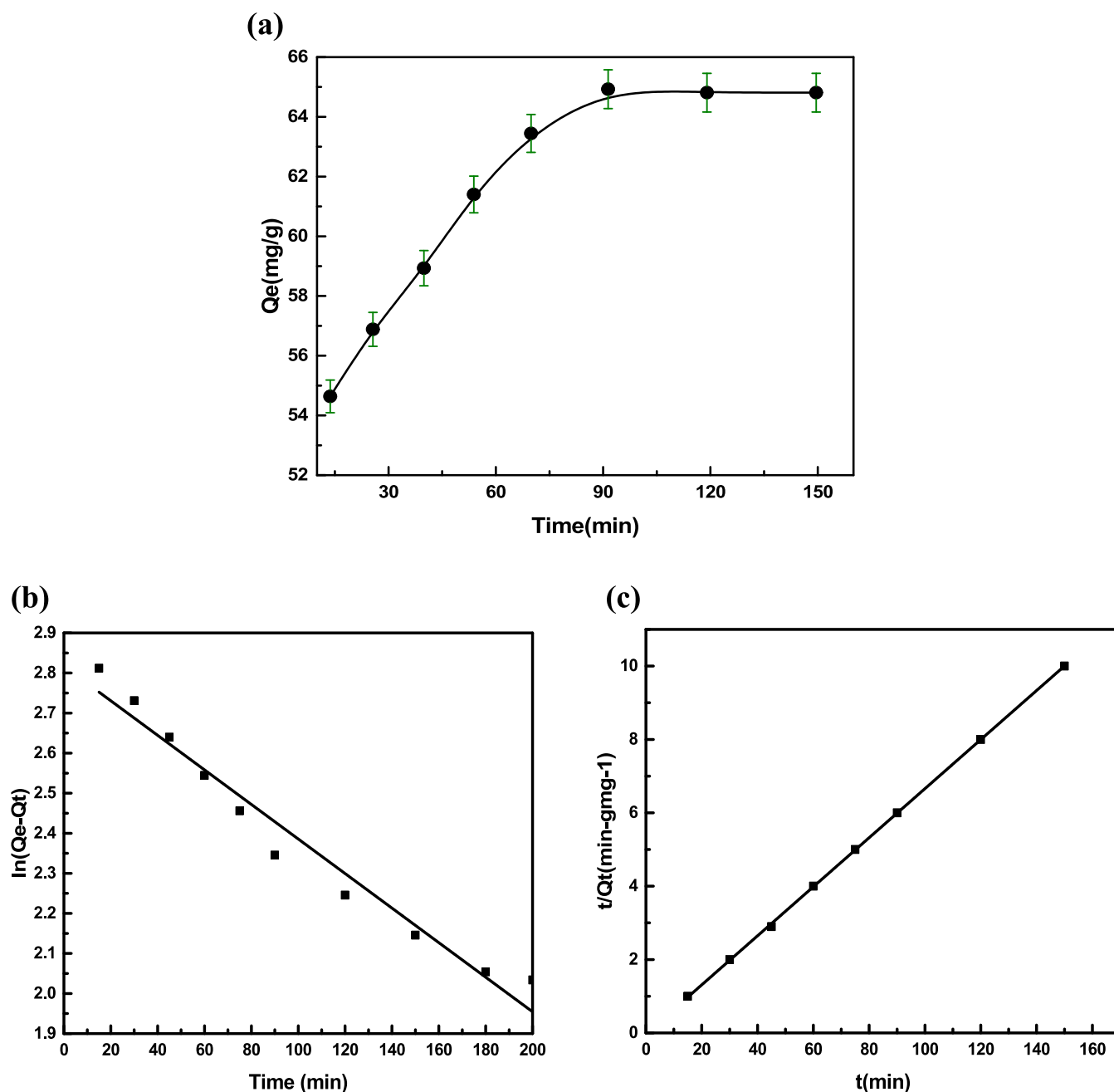


Figure 8. (a) Adsorption kinetic profiles of Cu(II) ions by VMBF-g-PGMA-S ($C_0 = 20 \text{ mg L}^{-1}$; mass = 15 mg; volume = 20 mL; and $T = 298 \text{ K}$). (b) Pseudo-first-order and (c) pseudo-second-order kinetic models for Cu(II) ion adsorption on VMBF-g-PGMA-S

Table 1. Kinetic Parameters of Cu(II) Ion Adsorption on VMBF-g-PGMA-S

	parameters	VMBF-g-PGMA-S
pseudo-1st-order	$k_1 \text{ (min}^{-1}\text{)}$	3.6×10^{-3}
	$Q_{\text{cal}} \text{ (mg}\cdot\text{g}^{-1}\text{)}$	16.94
	R^2	0.998
pseudo-2nd-order	$k_2 \text{ (mg}\cdot\text{g}^{-1}\cdot\text{min}^{-1}\text{)}$	1.02×10^{-2}
	$Q_{\text{cal}} \text{ (mg}\cdot\text{g}^{-1}\text{)}$	62.76
	R^2	0.999

maximum grafting on fibers occurred by the postpolymerization sulfonation method. The incorporation of GMA chains on VMBF-g-PGMA was established by FTIR spectroscopy, SEM, and XRD techniques. TGA was performed to analyze the

thermal stability of the synthesized fibers. The outcomes of the characterization techniques indicated that VMBF-g-PGMA-S was synthesized by consuming γ radiations. The results of the study indicated that at pH 5, a maximum of 96% adsorption of copper occurred. The resultant data from adsorption kinetics was more suitable for the PSO model with $R^2 = 0.999$. The isothermal study showed that the Langmuir model gives a better fit with experimental data, having $R^2 = 0.999$. Thermodynamic parameters were computed from thermodynamic studies at different temperatures, which shows the exothermic and spontaneous nature of the adsorption. The applicability of VMBF-g-PGMA-S for Cu(II) ion removal from wastewater was investigated. The results of these findings suggest that VMBF-g-PGMA-S opens a new avenue as a biosorbent for the cleaning of toxic metals from wastewater.

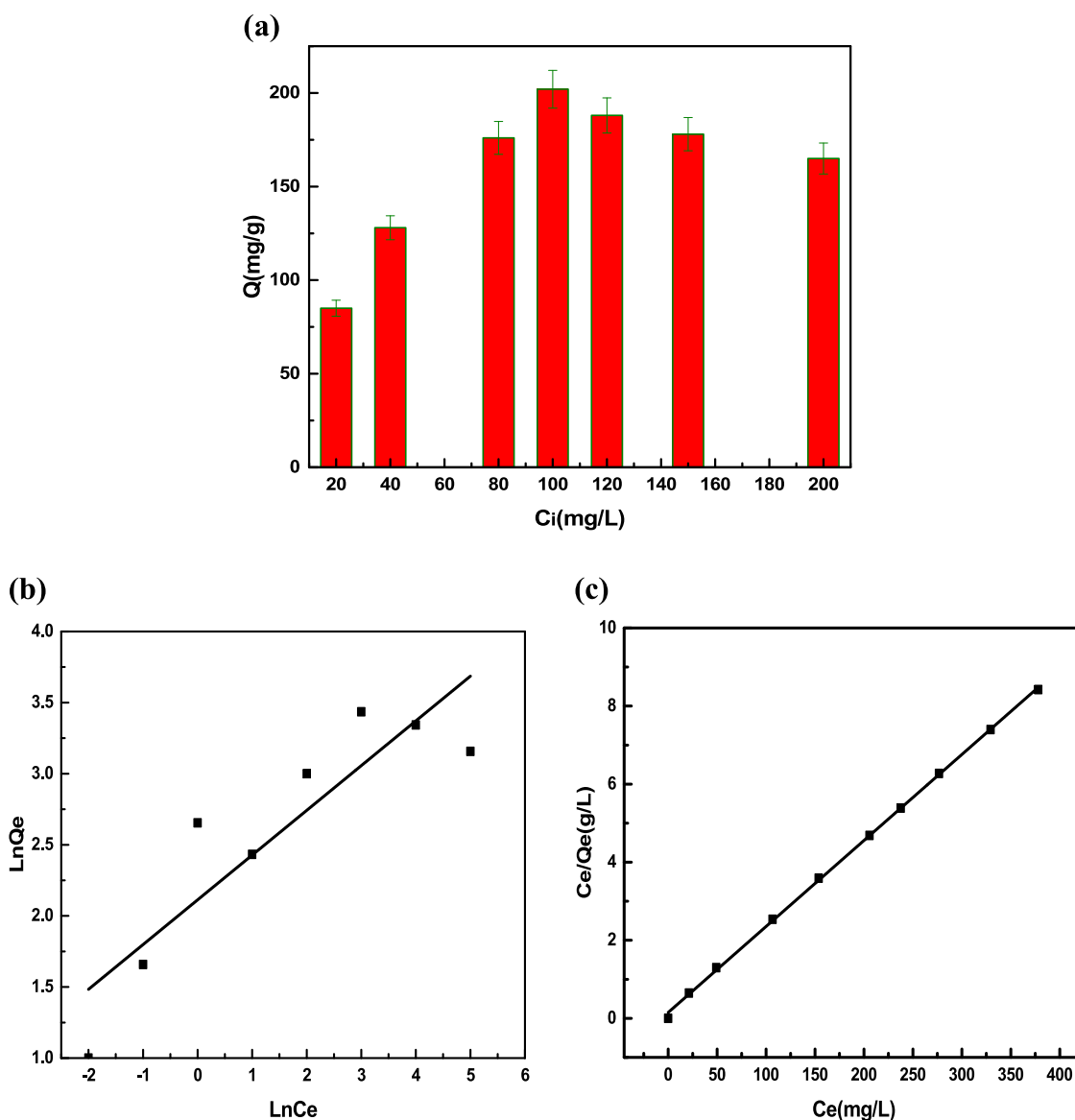


Figure 9. (a) Equilibrium adsorption capacity as a function of the initial concentration in the solutions. (b) Freundlich isotherm and (c) Langmuir isotherm models for Cu(II) ion adsorption on VMBF-g-PGMA-S

Table 2. Parameters of Isotherms for Cu(II) Ion Adsorption on VMBF-g-PGMA-S

isotherms	parameters	VMBF-g-PGMA-S'
Freundlich	n	2.186
	k_f	23.53
	R^2	0.757
Langmuir	Q_m	198
	K_L	7.14×10^{-3}
	R^2	0.999

Table 3. Thermodynamic Parameters of Cu(II) Ion Adsorption by VMBF-g-PGMA-S

temperature (K)	ΔG° (kJ mol ⁻¹)	ΔH° (kJ mol ⁻¹)	ΔS° (kJ mol ⁻¹ k ⁻¹)
283	-453.72	-26.97	3.81
293	-716.92		
303	-1198.65		

AUTHOR INFORMATION

Corresponding Author

Zarshad Ali – Department of Chemistry, Hazara University, Mansehra 21300, Pakistan; orcid.org/0000-0002-3253-2533; Phone: +92 997 414136; Email: zarshad11@yahoo.com; Fax: +92-997-530045

Authors

Ruqayya Shaheen – Department of Chemistry, Hazara University, Mansehra 21300, Pakistan; orcid.org/0009-0009-1320-7418

Tariq Yasin – Department of Chemistry, Pakistan Institute of Engineering and Applied Sciences (PIEAS), Islamabad 45650, Pakistan

Amir Sada Khan – Department of Chemistry, University of Science and Technology, Bannu 28100 Khyber Pakhtunkhwa, Pakistan

Bushra Adalat – Department of Chemistry, Hazara University, Mansehra 21300, Pakistan

Mehwish Tahir – Department of Chemistry, Pakistan Institute of Engineering and Applied Sciences (PIEAS), Islamabad 45650, Pakistan

Sher Bahadar Khan – Chemistry Department, Faculty of Science, King Abdulaziz University, Jeddah 21589, Saudi Arabia; orcid.org/0000-0001-9635-7175

Complete contact information is available at:

<https://pubs.acs.org/10.1021/acsomega.3c02466>

Notes

The authors declare no competing financial interest.

ACKNOWLEDGMENTS

The authors of this manuscript highly acknowledge the Pakistan Institute of Engineering and Applied Science (PIEAS) for providing the research facilities and expertise for this research.

REFERENCES

- (1) (a) Yadav, P.; Yadav, H.; Shah, V. G.; Shah, G.; Dhaka, G. Biomedical biopolymers, their origin and evolution in biomedical sciences: A systematic review. *J. Clin. Diagn. Res.* **2015**, *9* (9), ZE21–ZE25, DOI: [10.7860/JCDR/2015/13907.6565](https://doi.org/10.7860/JCDR/2015/13907.6565). (b) Dang, J. M.; Leong, K. W. Natural polymers for gene delivery and tissue engineering. *Adv. Drug Delivery Rev.* **2006**, *58* (4), 487–499.
- (2) (a) Kulkarni, V. S.; Butte, K. D.; Rathod, S. S. Natural polymers—A comprehensive review. *Int. J. Res. Pharm. Biomed. Sci.* **2012**, *3* (4), 1597–1613. (b) Ibrahim, M.; Sani, N.; Adamu, M.; Abubakar, M. Biodegradable polymers for sustainable environmental and economic development. *MOJ Biorg. Org. Chem.* **2018**, *2*, 192–194, DOI: [10.15406/mojboc.2018.02.00080](https://doi.org/10.15406/mojboc.2018.02.00080).
- (3) (a) Sun, Y.; Jing, X.; Ma, X.; Feng, Y.; Hu, H. Versatile types of polysaccharide-based drug delivery systems: From strategic design to cancer therapy. *Int. J. Mol. Sci.* **2020**, *21* (23), No. 9159, DOI: [10.3390/ijms21239159](https://doi.org/10.3390/ijms21239159). (b) Kaith, B. S.; Singha, A.; Kumar, S.; Kalia, S. Mercerization of flax fiber improves the mechanical properties of fiber-reinforced composites. *Int. J. Polym. Mater.* **2008**, *57* (1), 54–72.
- (4) Raza, A.; Tahir, M.; Nasir, A.; Yasin, T.; Nadeem, M. Sepiolite grafted polypyrrole: Influence of degree of grafting on structural, thermal, and impedance properties of nanohybrid. *J. Appl. Polym. Sci.* **2020**, *137* (37), No. 49085, DOI: [10.1002/app.49085](https://doi.org/10.1002/app.49085).
- (5) Bucio, E.; Burillo, G. Radiation-induced grafting of sensitive polymers. *J. Radioanal. Nucl. Chem.* **2009**, *280* (2), 239–243.
- (6) (a) Kumar, V.; Bhardwaj, Y.; Rawat, K.; Sabharwal, S. Radiation-induced grafting of vinylbenzyltrimethylammonium chloride (VBT) onto cotton fabric and study of its anti-bacterial activities. *Radiat. Phys. Chem.* **2005**, *73* (3), 175–182. (b) Seko, N.; Bang, L.; Tamada, M. Syntheses of amine-type adsorbents with emulsion graft polymerization of glycidyl methacrylate. *Nucl. Instrum. Methods Phys. Res., Sect. B* **2007**, *265* (1), 146–149.
- (7) Chaudhari, C.; Guin, J. P.; Dubey, K.; Bhardwaj, Y.; Varshney, L. Radiation induced grafting of glycidyl methacrylate on Teflon scrap for synthesis of dual type adsorbent: Process parameter standardisation. *Environ. Prog. Sustainable Energy* **2016**, *35* (5), 1367–1373.
- (8) (a) Seko, N.; Ninh, N. T. Y.; Tamada, M. Emulsion grafting of glycidyl methacrylate onto polyethylene fiber. *Radiat. Phys. Chem.* **2010**, *79* (1), 22–26. (b) Zheng, T.; Zhang, Z.; Shukla, S.; Agnihotri, S.; Clemons, C. M.; Pilla, S. PHBV-graft-GMA via reactive extrusion and its use in PHBV/nanocellulose crystal composites. *Carbohydr. Polym.* **2019**, *205*, 27–34.
- (9) Elkady, M.; Abu-Saied, M.; Rahman, A. A.; Soliman, E.; Elzatahry, A.; Yossef, M. E.; Eldin, M. M. Nano-sulphonated poly (glycidyl methacrylate) cations exchanger for cadmium ions removal: effects of operating parameters. *Desalination* **2011**, *279* (1–3), 152–162.
- (10) Huš, S.; Kolar, M.; Krajnc, P. Separation of heavy metals from water by functionalized glycidyl methacrylate poly (high internal phase emulsions). *J. Chromatogr. A* **2016**, *1437*, 168–175.
- (11) Lv, H.; Zhang, W.; Hosseini, M.; Samani, M. R.; Toghraie, D. Characterization and synthesis of new adsorbents with some natural waste materials for the purification of aqueous solutions. *J. Environ. Manage.* **2023**, *336*, No. 117660.
- (12) (a) Shih, Y.-F.; Cai, J.-X.; Kuan, C.-S.; Hsieh, C.-F. Plant fibers and wasted fiber/epoxy green composites. *Composites, Part B* **2012**, *43* (7), 2817–2821. (b) Liew, F. K.; Hamdan, S.; Rahman, M.; Rusop, M. Thermomechanical properties of jute/bamboo cellulose composite and its hybrid composites: the effects of treatment and fiber loading. *Adv. Mater. Sci. Eng.* **2017**, *2017*, No. 8630749, DOI: [10.1155/2017/8630749](https://doi.org/10.1155/2017/8630749).
- (13) Wang, C.; Zuo, Q.; Lin, T.; Anuar, N. I. S.; Salleh, K. M.; Gan, S.; Yousfani, S. H. S.; Zuo, H.; Zakaria, S. Predicting thermal conductivity and mechanical property of bamboo fibers/polypropylene nonwovens reinforced composites based on regression analysis. *Int. Commun. Heat Mass Transfer* **2020**, *118*, No. 104895.
- (14) Teli, M.; Sheikh, J. Grafting of bamboo rayon with acrylic acid and its effect on cationic dyeing. *Cellul. Chem. Technol.* **2012**, *46*, 53–59.
- (15) Cichosz, S.; Masek, A.; Wolski, K.; Zaborski, M. Universal approach of cellulose fibres chemical modification result analysis via commonly used techniques. *Polym. Bull.* **2019**, *76* (5), 2147–2162.
- (16) Amin, M. T.; Alazba, A.; Manzoor, U. A review of removal of pollutants from water/wastewater using different types of nanomaterials. *Adv. Mater. Sci. Eng.* **2014**, *2014*, No. 825910, DOI: [10.1155/2014/825910](https://doi.org/10.1155/2014/825910).
- (17) Babu, R. S.; Prasanna, K.; Kumar, P. S. A censorious review on the role of natural lignocellulosic fiber waste as a low-cost adsorbent for removal of diverse textile industrial pollutants. *Environ. Res.* **2022**, *215*, No. 114183, DOI: [10.1016/j.envres.2022.114183](https://doi.org/10.1016/j.envres.2022.114183).
- (18) Ali, H.; Khan, E.; Sajad, M. A. Phytoremediation of heavy metals—concepts and applications. *Chemosphere* **2013**, *91* (7), 869–881.
- (19) Dang, X.; Yu, Z.; Yang, M.; Woo, M. W.; Song, Y.; Wang, X.; Zhang, H. Sustainable electrochemical synthesis of natural starch-based biomass adsorbent with ultrahigh adsorption capacity for Cr (VI) and dyes removal. *Sep. Purif. Technol.* **2022**, *288*, No. 120668.
- (20) Alasadi, A.; Khaili, F.; Awwad, A. Adsorption of Cu (II), Ni (II) and Zn (II) ions by nano kaolinite: Thermodynamics and kinetics studies. *Chem. Int.* **2019**, *5* (4), 258–326.
- (21) Tahir, M.; Raza, A.; Nasir, A.; Yasin, T. Radiation induced graft polymerization of glycidyl methacrylate onto sepiolite. *Radiat. Phys. Chem.* **2021**, *179*, No. 109259.
- (22) Flores-Rojas, G.; López-Saucedo, F.; Bucio, E. Gamma-irradiation applied in the synthesis of metallic and organic nanoparticles: a short review. *Radiat. Phys. Chem.* **2020**, *169*, No. 107962.
- (23) Taimur, S.; Hassan, M.; Yasin, T. Removal of copper using novel amidoxime based chelating nanohybrid adsorbent. *Eur. Polym. J.* **2017**, *95*, 93–104.
- (24) Omichi, M.; Ueki, Y.; Seko, N.; Maekawa, Y. Development of a simplified radiation-induced emulsion graft polymerization method and its application to the fabrication of a heavy metal adsorbent. *Polymers* **2019**, *11* (8), No. 1373, DOI: [10.3390/polym11081373](https://doi.org/10.3390/polym11081373).
- (25) Khan, I. A.; Hussain, H.; Yasin, T.; Inaam-ul-Hassan, M. Surface modification of mesoporous silica by radiation induced graft polymerization of styrene and subsequent sulfonation for ion-exchange applications. *J. Appl. Polym. Sci.* **2020**, *137* (26), No. 48835, DOI: [10.1002/app.48835](https://doi.org/10.1002/app.48835).
- (26) Martijanti, M.; Juwono, A.; Sutarno, S. Investigation of characteristics of bamboo fiber for composite structures. *IOP Conf. Ser.: Mater. Sci. Eng.* **2020**, *850*, No. 012028, DOI: [10.1088/1757-899x/850/1/012028](https://doi.org/10.1088/1757-899x/850/1/012028).
- (27) Liew, F. K.; Hamdan, S.; Rahman, M.; Rusop, M.; Lai, J. C. H.; Hossen, M.; Rahman, M. M. Synthesis and characterization of cellulose from green bamboo by chemical treatment with mechanical

- process. *J. Chem.* **2015**, *2015*, No. 212158, DOI: 10.1155/2015/212158.
- (28) Song, X.-Y.; Wang, M.; Weng, Y.-X.; Huang, Z.-G. Effect of bamboo flour grafted lactide on the interfacial compatibility of polylactic acid/bamboo flour composites. *Polymers* **2017**, *9* (8), No. 323, DOI: 10.3390/polym9080323.
- (29) Abu-Saied, M. A.; Fontananova, E.; Drioli, E.; Eldin, M. Sulphonated poly (glycidyl methacrylate) grafted cellophane membranes: novel application in polyelectrolyte membrane fuel cell (PEMFC). *J. Polym. Res.* **2013**, *20* (7), No. 187, DOI: 10.1007/s10965-013-0187-4.
- (30) Kang, P. H.; Jeun, J. P.; Chung, B. Y.; Kim, J. S.; Nho, Y. C. Preparation and characterization of glycidyl methacrylate (GMA) grafted kapok fiber by using radiation induced-grafting technique. *J. Ind. Eng. Chem.* **2007**, *13* (6), 956–958.
- (31) Lin, J.; Yang, Z.; Hu, X.; Hong, G.; Zhang, S.; Song, W. The effect of alkali treatment on properties of dopamine modification of bamboo fiber/polylactic acid composites. *Polymers* **2018**, *10* (4), No. 403, DOI: 10.3390/polym10040403.
- (32) Thakur, M. K.; Gupta, R. K.; Thakur, V. K. Surface modification of cellulose using silane coupling agent. *Carbohydr. Polym.* **2014**, *111*, 849–855.
- (33) Madrid, J. F.; Abad, L. V. Modification of microcrystalline cellulose by gamma radiation-induced grafting. *Radiat. Phys. Chem.* **2015**, *115*, 143–147.
- (34) (a) Luo, J.; Semenikhin, N.; Chang, H.; Moon, R. J.; Kumar, S. Post-sulfonation of cellulose nanofibrils with a one-step reaction to improve dispersibility. *Carbohydr. Polym.* **2018**, *181*, 247–255. (b) Guo, L.; Meng, A.; Wang, L.; Huang, J.; Wang, X.; Ren, H.; Zhai, H.; Ek, M. Improving the compatibility, surface strength, and dimensional stability of cellulosic fibers using glycidyl methacrylate grafting. *J. Mater. Sci.* **2020**, *55* (27), 12906–12920.
- (35) Hu, Z.; Zhai, R.; Li, J.; Zhang, Y.; Lin, J. Preparation and characterization of nanofibrillated cellulose from bamboo fiber via ultrasonication assisted by repulsive effect. *Int. J. Polym. Sci.* **2017**, *2017*, No. 9850814, DOI: 10.1155/2017/9850814.
- (36) Nasir, A.; Raza, A.; Tahir, M.; Yasin, T. Free-radical graft polymerization of acrylonitrile on gamma irradiated graphene oxide: Synthesis and characterization. *Mater. Chem. Phys.* **2020**, *246*, No. 122807.
- (37) ul Hassan, M. I.; Taimur, S.; Khan, I. A.; Yasin, T.; Ali, S. W. Surface modification of polypropylene waste by the radiation grafting of styrene and upcycling into a cation-exchange resin. *J. Appl. Polym. Sci.* **2019**, *136* (10), No. 47145, DOI: 10.1002/app.47145.
- (38) Johar, N.; Ahmad, I.; Dufresne, A. Extraction, preparation and characterization of cellulose fibres and nanocrystals from rice husk. *Ind. Crops Prod.* **2012**, *37* (1), 93–99.
- (39) Chen, H.; Zhang, W.; Wang, X.; Wang, H.; Wu, Y.; Zhong, T.; Fei, B. Effect of alkali treatment on wettability and thermal stability of individual bamboo fibers. *J. Wood Sci.* **2018**, *64* (4), 398–405.
- (40) Elemike, E. E.; Onwudiwe, D.; Ivwurie, W. Structural and thermal characterization of cellulose and copper oxide modified cellulose obtained from bamboo plant fibre. *SN Appl. Sci.* **2020**, *2* (10), No. 1725, DOI: 10.1007/s42452-020-03503-6.
- (41) Ma, H.; Morita, K.; Hoshina, H.; Seko, N. Synthesis of amine-type adsorbents with emulsion graft polymerization of 4-hydroxybutyl acrylate glycidylether. *Mater. Sci. Appl.* **2011**, *02* (07), 776–784, DOI: 10.4236/msa.2011.27107.
- (42) Singha, A.; Guleria, A. Chemical modification of cellulosic biopolymer and its use in removal of heavy metal ions from wastewater. *Int. J. Biol. Macromol.* **2014**, *67*, 409–417.
- (43) ul Hassan, M. I.; Taimur, S.; Yasin, T. Upcycling of polypropylene waste by surface modification using radiation-induced grafting. *Appl. Surf. Sci.* **2017**, *422*, 720–730.
- (44) Hajeeth, T.; Vijayalakshmi, K.; Gomathi, T.; Sudha, P.; Anbalagan, S. Adsorption of copper (II) and nickel (II) ions from aqueous solution using graft copolymer of cellulose extracted from the sisal fiber with acrylic acid monomer. *Compos. Interfaces* **2014**, *21* (1), 75–86.
- (45) Tirtom, V. N.; Dinçer, A.; Becerik, S.; Aydemir, T.; Çelik, A. Removal of lead (II) ions from aqueous solution by using crosslinked chitosan-clay beads. *Desalin. Water Treat.* **2012**, *39* (1–3), 76–82.
- (46) Çelebi, H. Use of Bioballs as an Adsorbent for the Removal of Copper. *J. Chem. Soc. Pak.* **2021**, *43* (2), No. 114, DOI: 10.52568/000565.
- (47) Batool, F.; Akbar, J.; Iqbal, S.; Noreen, S.; Bukhari, S. N. A. Study of isothermal, kinetic, and thermodynamic parameters for adsorption of cadmium: an overview of linear and nonlinear approach and error analysis. *Bioinorg. Chem. Appl.* **2018**, *2018*, No. 3463724, DOI: 10.1155/2018/3463724.
- (48) Ho, Y.-S. Review of second-order models for adsorption systems. *J. Hazard. Mater.* **2006**, *136* (3), 681–689.
- (49) Tong, K.; Kassim, M. J.; Azraa, A. Adsorption of copper ion from its aqueous solution by a novel biosorbent *Uncaria gambir*: Equilibrium, kinetics, and thermodynamic studies. *Chem. Eng. J.* **2011**, *170* (1), 145–153.
- (50) Kumar, R.; Sharma, R. K.; Singh, A. P. Sorption of Ni (II), Pb (II) and Cu (II) ions from aqueous solutions by cellulose grafted with poly (HEMA-co-AAc): kinetic, isotherm and thermodynamic study. *J. Environ. Chem. Eng.* **2019**, *7* (3), No. 103088.
- (51) Ozsoy, H. D.; Kumbur, H. Adsorption of Cu (II) ions on cotton boll. *J. Hazard. Mater.* **2006**, *136* (3), 911–916.
- (52) Desta, M. B. Batch sorption experiments: Langmuir and Freundlich isotherm studies for the adsorption of textile metal ions onto teff straw (*Eragrostis tef*) agricultural waste. *J. Thermodyn.* **2013**, *2013*, No. 375830, DOI: 10.1155/2013/375830.
- (53) El-Bahy, S. M.; El-Bahy, Z. M. Synthesis and characterization of polyamidoxime chelating resin for adsorption of Cu (II), Mn (II) and Ni (II) by batch and column study. *J. Environ. Chem. Eng.* **2016**, *4* (1), 276–286.
- (54) Al-Karawi, A. J. M.; Al-Qaisi, Z. H. J.; Abdullah, H. I.; Al-Mokaram, A. M. A.; Al-Heetimi, D. T. A. Synthesis, characterization of acrylamide grafted chitosan and its use in removal of copper (II) ions from water. *Carbohydr. Polym.* **2011**, *83* (2), 495–500.
- (55) Piccin, J.; Dotto, G.; Pinto, L. Adsorption isotherms and thermochemical data of FD&C Red n 40 binding by chitosan. *Braz. J. Chem. Eng.* **2011**, *28*, 295–304.